

Biomass burning emissions of reactive gases estimated from satellite data analysis and ecosystem modeling for the Brazilian Amazon region

Christopher Potter

NASA Ames Research Center, Moffett Field, California, USA

Vanessa Brooks-Genovese, Steven Klooster, and Alicia Torregrosa

Earth System Science and Policy, California State University Monterey Bay, Seaside, California, USA

Received 11 December 2000; revised 30 April 2001; accepted 26 June 2001; published XX Month 2002.

[1] To produce a new daily record of trace gas emissions from biomass burning events for the Brazilian Legal Amazon, we have combined satellite advanced very high resolution radiometer (AVHRR) data on fire counts together for the first time with vegetation greenness imagery as inputs to an ecosystem biomass model at 8 km spatial resolution. This analysis goes beyond previous estimates for reactive gas emissions from Amazon fires, owing to a more detailed geographic distribution estimate of vegetation biomass, coupled with daily fire activity for the region (original 1 km resolution), and inclusion of fire effects in extensive areas of the Legal Amazon (defined as the Brazilian states of Acre, Amapá, Amazonas, Maranhao, Mato Grosso, Pará, Rondônia, Roraima, and Tocantins) covered by open woodland, secondary forests, savanna, and pasture vegetation. Results from our emissions model indicate that annual emissions from Amazon deforestation and biomass burning in the early 1990s total to 102 Tg yr⁻¹ carbon monoxide (CO) and 3.5 Tg yr⁻¹ nitrogen oxides (NO_x). Peak daily burning emissions, which occurred in early September 1992, were estimated at slightly more than 3 Tg d⁻¹ for CO and 0.1 Tg d⁻¹ for NO_x flux to the atmosphere. Other burning source fluxes of gases with relatively high emission factors are reported, including methane (CH₄), nonmethane hydrocarbons (NMHC), and sulfur dioxide (SO₂), in addition to total particulate matter (TPM). We estimate the Brazilian Amazon region to be a source of between one fifth and one third for each of these global emission fluxes to the atmosphere. The regional distribution of burning emissions appears to be highest in the Brazilian states of Maranhao and Tocantins, mainly from burning outside of moist forest areas, and in Pará and Mato Grosso, where we identify important contributions from primary forest cutting and burning. These new daily emission estimates of reactive gases from biomass burning fluxes are designed to be used as detailed spatial and temporal inputs to computer models and data analysis of tropospheric chemistry over the tropical region. *INDEX TERMS:* 1610 Global Change: Atmosphere (0315, 0325); 1615 Global Change: Biogeochemical processes (4805)

1. Introduction

[2] Biomass burning emissions of gases such as carbon dioxide, carbon monoxide, methane, nitrogen oxides, hydrocarbons, and particulate matter can affect atmospheric chemistry, and possibly regional and global climate [Crutzen and Andreae, 1990; Galanter *et al.*, 2000]. Among the major components necessary for understanding air pollution impacts on the global atmosphere, few are as uncertain as the rates and impacts of tropical biomass burning fluxes of trace gases and emission of smoke aerosols. The tropical regions have been identified as a probable net source of carbon to the atmosphere, chiefly because of high deforestation rates and frequency of fires [Hao and Lui, 1994; Ciais *et al.*, 1995; Potter, 1999]. The added effects of smoke

emissions from vegetation fires on ozone sources, radiation fluxes, cloud microstructure, and rainfall patterns are of major concern on regional scales [Kaufman *et al.*, 1998].

[3] Ozone (O₃) is produced in the troposphere by the photochemical oxidation of CO and hydrocarbons in the presence of NO_x. In the tropical zones, transport of O₃ from the stratosphere into the troposphere is relatively small compared to the rate of in situ photochemical production from emission precursors [Jacob *et al.*, 1996; Thompson *et al.*, 1996], such as those from biomass burning. Furthermore, most of the global oxidation of the long-lived, radiatively and chemically important trace gases may take place in the tropical atmosphere [Crutzen, 1995]. Changes in the budgets of O₃, NO_x, CO, CH₄, and NMHC may cause significant changes in the oxidizing power of the global atmosphere and possibly alter the budgets of the long-lived trace gases as well. In addition, aerosols generated from vegetation fires can have widespread influence on the

radiative and chemical properties of the atmosphere not only over the Amazon region itself but also on global scales [Artaxo *et al.*, 1988].

[4] Despite concerted efforts to monitor major burning activities throughout Brazil [Setzer and Pereira, 1991; Prins *et al.*, 1998; Alves, 1999; Nepstad *et al.*, 1999], there is still no long term (>5 years), high resolution (<0.5°) mapping record for daily biomass burning emissions of CO₂ and other reactive trace gases over the Amazon region. Major gaps in data access and information remain in terms of the precise location, size, and timing (hourly to daily) of fires in the Amazon, as well as in amounts of vegetation biomass potentially subjected to burning and in the type of burning that occurs from one locality to the next. This means that there is only indirect evidence of the actual contribution of biomass burning to pollutant gas emission to the atmosphere over the largest tropical forest region of the world.

[5] The gas composition of biomass burning emissions is a function of two major factors: (1) the elemental composition (carbon, nitrogen, sulfur, etc.) of the biomass subject to burning and (2) the relative contribution of flaming and smoldering combustion processes during a burn. Trace gas emissions from the burning of natural vegetation are a mixture of compounds that originate from flaming and smoldering processes, with different proportions depending on the type of fire. For example, most savanna vegetation is consumed in the flaming stage, whereas forest biomass is combusted about equally by both processes [Lobert *et al.*, 1991]. Relatively oxidized compounds, such as CO₂, NO, NO₂, SO₂, N₂O and elemental carbon particles, are commonly emitted during the flaming stage of a fire. A high proportion of emission of more reduced compounds (CO, CH₄, nonmethane hydrocarbons, PAH, NH₃, HCN, CH₃CN, amines, CH₃Cl, H₂S, COS, DMS, and organic particles) can occur during the smoldering stage [Yokelson *et al.*, 1997]. Consequently, it is crucial for regional scale studies of atmospheric chemistry to characterize localized burning sources with respect to not only amounts of biomass potentially consumed in a fire but also by the type of biomass (e.g., woody versus nonwoody) present for major vegetation types.

[6] A central objective of most international biosphere research programs is to characterize and quantify the global and regional production of chemically and radiatively important gases and aerosol species from biomass burning sources. In this study we have generated new high resolution predictions of daily trace gas emission for the Brazilian Amazon region, based on a combination of satellite fire counts from the Global Fire Product [Stroppiana *et al.*, 2000] and vegetation biomass pools from the NASA-CASA (Carnegie–Ames–Stanford Approach) model [Potter and Klooster, 1997, 1999b; Potter, 1999]. The NASA-CASA model includes interactions of several key controls on net ecosystem production (NEP) of carbon and total biomass in the tropics: surface radiation fluxes, evapotranspiration and soil water balance, soil fertility, and microbial activity affecting decomposition of plant residues. Regional scaling is accomplished by merging input data sets from satellite advanced very high resolution radiometer (AVHRR), surface climate, radiation, vegetation, and soils with model algorithms for carbon and moisture flow and energy use

processes in terrestrial ecosystems. Global satellite observations to drive the NASA-CASA model are an important feature for improving current burning-derived trace gas emissions, because (1) satellite images provide consistent, relatively high temporal and spatial resolution for land surface processes, (2) predicted biomass accumulation by vegetation types are formulated to be consistent with the range of measured rates from field studies worldwide, and (3) actual regional patterns for land cover attributes, such as biomass of forests, may differ substantially from potential vegetation maps or from extrapolation using a small set of sparsely distributed site measurements.

2. Biomass Burning Emission Algorithm

[7] The general method used in this study to compute biomass burning gas emissions is based on the approach described by Potter *et al.* [2001a]. To estimate regional trace gas emissions from vegetation fires, we apply the following equation derived originally from Seiler and Crutzen [1980]:

$$E_t = \sum_x B(x) C_F e_f A(x, t) \quad (1)$$

where E_t (Tg) is the regional emissions total at time t (d), B is the biomass subjected to burn at location x (e.g., 8 km grid cell), C_F is the biomass combustion fraction associated with a particular plant tissue fraction (leaf versus wood), e_f is the emission factor (flaming and/or smoldering) associated with a particular trace gas, A is the area burned at location x and time t .

[8] To estimate the B term in equation (1), maps of vegetation biomass can be derived by one of two general methods. The first is by spatial interpolation, using what is normally a small number (<100) of intensive field site measurements of aboveground plant mass [Houghton *et al.*, 2000]. A weakness of any interpolation method is that a small number of measurements may not adequately represent the variability of biomass growth patterns, especially over a vast region like the Amazon. The second general method, and the one used in this study, is developed through a combination of satellite remote sensing and ecosystem carbon flux modeling. Satellite imagery can be transformed using plant production models to provide relatively high spatial resolution maps of aboveground biomass over a regional area of interest [Potter *et al.*, 2001a]. Ecosystem models can readily incorporate climate, radiation, soils, and land use effects on plant growth that may be represented in a combination of georegistered information layers.

[9] The e_f term in equation (1) is defined as the amount of a compound released per amount of fuel consumed (g dry matter). Uncertainties associated with e_f for important trace gas species such as CO and CH₄ are generally in the range of 20–30% [Lobert *et al.*, 1991]. Calculation of this parameter requires knowledge of the carbon content of the biomass burned and the carbon budget of the fire usually expressed as the C_F term [Ward *et al.*, 1996]. Where fuel and residue data at the ground level are not available, an overall fuel carbon content of 45% is commonly assumed [Seiler and Crutzen, 1980].

[10] The A term in equation (1) can be estimated either through collating ground survey information or, as in this

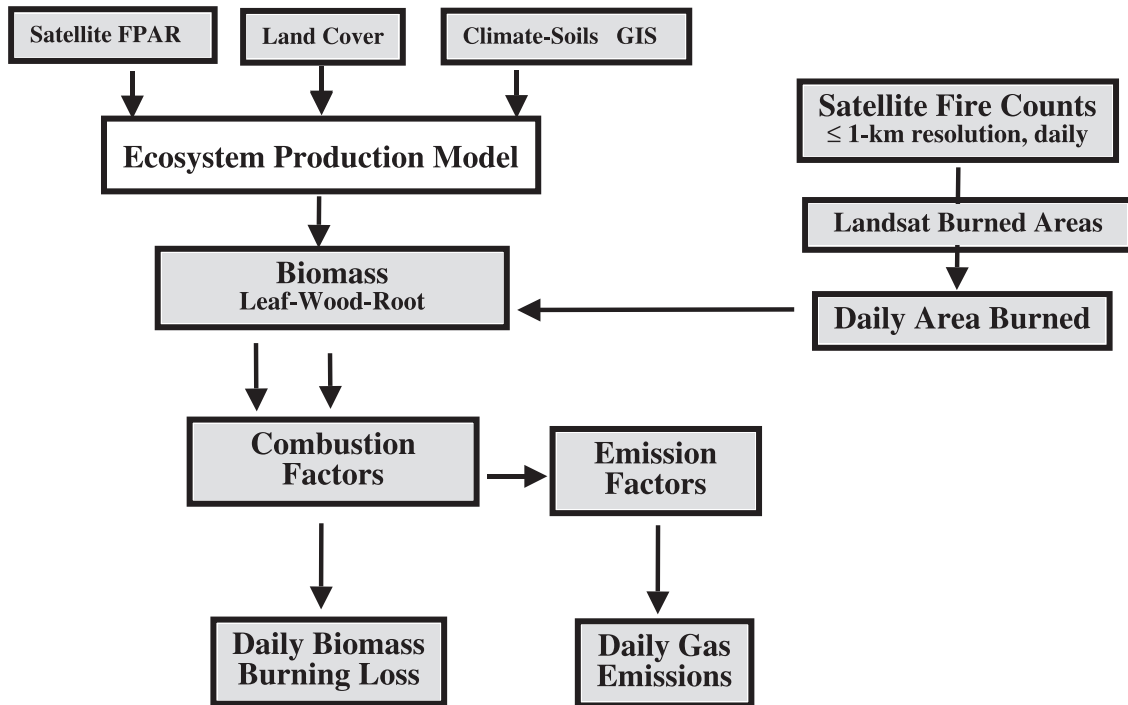


Figure 1. Flowchart of data transformations and modeling steps for regional estimates of biomass burning emissions.

study, through satellite remote sensing of fire activity. Once properly calibrated and adjusted for possible contamination effects, satellite fire counts provide a consistent method of identifying days and precise areas of relatively high burning activity. In the sections of this paper that follow, methods for estimating each term in equation (1) are described in more detail. A flowchart diagram of all major data and modeling steps is shown in Figure 1.

2.1. Biomass Modeling Methods

[11] A complete description of the previous NASA-CASA model design for regional carbon cycling in Amazon ecosystems is provided by *Potter et al.* [1998, 2001b], including the method to estimate net primary production (NPP) as a product of cloud-corrected solar surface irradiance (S), fractional intercepted photosynthetically active radiation (FPAR), and a maximum light use efficiency term (ϵ), modified by normalized temperature (T) and moisture (W) stress scalars (equation (2)).

$$NPP = S \text{ FPAR } \epsilon T W \quad (2)$$

[12] In the regional simulation mode, estimation of FPAR comes from a normalized difference vegetation index derived from AVHRR channel 1 (0.5–0.68 μm , visible) and channel 2 (0.73–1.1 μm , near IR) reflectance values [*Potter et al.*, 1993; *Sellers et al.*, 1994]. Predictions of changes in monthly soil moisture and evapotranspiration fluxes are 8 km resolution outputs of the NASA-CASA model. The W stress term is computed on the basis of the predicted monthly ratio of estimated evapotranspiration (EET) to potential evapotranspiration (PET) [*Priestly and Taylor*, 1972].

[13] Regional data sets (8 km resolution) from a geographic information system (GIS) are used as model climate drivers and land surface parameter files. We assembled a complete set of coregistered GIS raster coverages to serve as model-compatible inputs, including interpolated monthly (1982–1990) rainfall records from Brazil’s Departamento Nacional de Aguas e Energia Eletrica (DNAEE) network, surface air temperature [*New et al.*, 2000], surface solar radiation (from the International Satellite Cloud Climatology Program [*Bishop and Rossow*, 1991]), soil type and texture from RADAMBRASIL [*Ministério das Minas e Energia (MME)*, 1981; *Potter et al.*, 1998], land cover type (from AVHRR and Landsat classification [*Stone et al.*, 1994]), and NASA’s AVHRR Pathfinder satellite vegetation index [*Agbu and James*, 1994] for the country of Brazil and, in some cases, for the larger Amazon region. Methods to generate 8 km resolution climate driver variables for the NASA-CASA biomass estimates over the Amazon region are documented thoroughly by *Potter et al.* [2001b]. All climate inputs to the model were developed and validated using spatial interpolations of gridded historical station measurements, in lieu of a regional climate model.

[14] Because of cloud cover and smoke-aerosol interference, which can be prevalent at different times and locations in the Amazon region, we applied Fourier smoothing algorithms (FA) developed by *Los et al.* [1994] for AVHRR data sets to further remove erroneous atmospheric signals in the satellite greenness index. Application of the FA algorithm modified mean annual index values by more than +10% of their original values in approximately 4 out of every 10 grid cells in the region [*Potter et al.*, 1998].

[15] Our aboveground biomass estimation methods do not derive directly from optical remote sensing (e.g., the

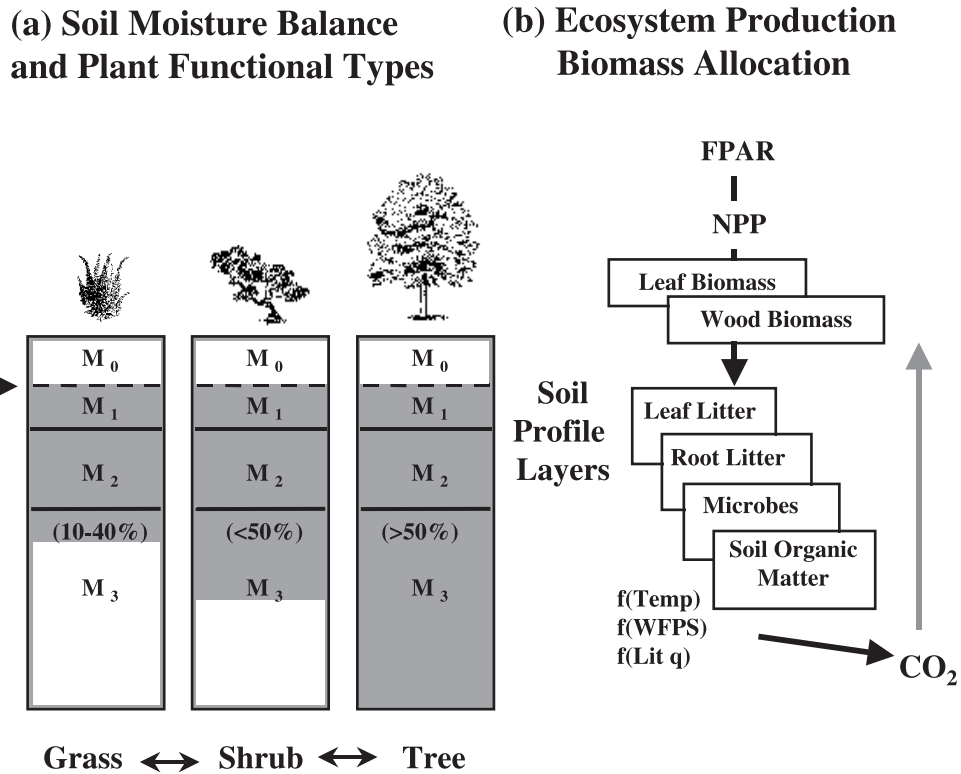


Figure 2. Structure of the NASA-CASA model. (a) Typical soil water balance is shown as the shaded depth level in soil profile layers [M₁–M₃] for major plant functional types [PFTs]: for example, deserts, grasses, and overstory woody plants [shrubs and trees]. (b) Climate controls on net primary production [NPP] are defined in equation (2), including fraction of absorbed photosynthetically active radiation [FPAR], precipitation [PPT], and potential evapotranspiration [PET]. Controls on litter and soil C decomposition are defined as soil temperature [Temp], water-filled pore space [WFPS], and nitrogen/lignin content [Lit q].

AVHRR) but are based rather on multi-year inputs of NPP from satellite data using well-documented methods previously described [Potter *et al.*, 1993; Sellers *et al.*, 1994]. Biomass is subsequently estimated as a function of residence times and allocation rates in our ecosystem simulation model (Figure 2). Carbon and nitrogen allocation among leaf, wood, and fine root tissues from NPP (Table 1) are defined as a set of fractional allocation constants of plant tissue pools (α) and the mean residence time (τ , in years) of carbon in the standing plant tissue pools [Terborgh *et al.*, 1997; Potter and Klooster, 1999a]. Soil fertility effects are included in this model version to adjust these allocation constants for generalized nutrient limitations. We classified soil types in the Soil Map of Brazil [MME, 1981] according to three relative levels of soil fertility (low, medium, and high) [Potter *et al.*, 2001b]. On low-fertility soils, an adjustment (+10%) is favored that allocates increasing root biomass for the acquisition of soil nutrients [Wilson and Tilman, 1991]. On medium-to-high fertility soils, a similar adjustment is favored that allocates 10% more to above-ground wood and leaf biomass for light harvesting functions in the canopy [Gleeson and Tilman, 1990; Redente *et al.*, 1992; Lusk *et al.*, 1997].

[16] To more accurately represent climate controls and soil processes for Amazon ecosystem carbon cycling, several modifications are introduced in this study for the

Amazon version of the NASA-CASA model (Figure 2) described by Potter *et al.* [2001b]. These changes include refinement of water balance equations, moisture holding and retention capacity for Amazon soils. The soil profile is treated as a series of four layers: ponded surface water, surface organic matter, topsoil (0.3 m), and subsoil to rooting depth (1–10 m). These layers can differ in soil texture, moisture-holding capacity, and carbon-cycling dynamics. Soil water retention curves were designed to reflect the hybrid character of Amazon oxisols, which

Table 1. Allocation and Residence Time Parameters for Major Vegetation Types, Following Global Cover Classes Defined by Defries and Townshend [1994]^a

Vegetation Type	α_{Leaf}	α_{Root}	α_{Wood}	τ_{Leaf}	τ_{Root}	τ_{Wood}
Annual grassland and crops	0.45	0.55	...	1.5	5.0	...
Mixed deciduous forest	0.30	0.25	0.45	1.0	3.0	40
Desert and bare ground	0.25	0.25	0.50	1.5	3.0	50
Semiarid shrub land	0.25	0.25	0.50	1.5	3.0	50
Savanna and wooded grassland	0.30	0.25	0.45	1.0	5.0	25
Tropical evergreen rain forest	0.25	0.25	0.50	1.5	2.0	25

^a Alpha (α) is the proportional allocation constant of plant tissue pools; τ is the residence time (in years) of carbon in plant tissue pools. Sources for information on parameter settings include Cannell [1982], Aber and Melillo [1991], Running and Gower [1991], Redente *et al.* [1992], Lusk *et al.* [1997], Terborgh *et al.* [1997], and Guild *et al.* [1998].

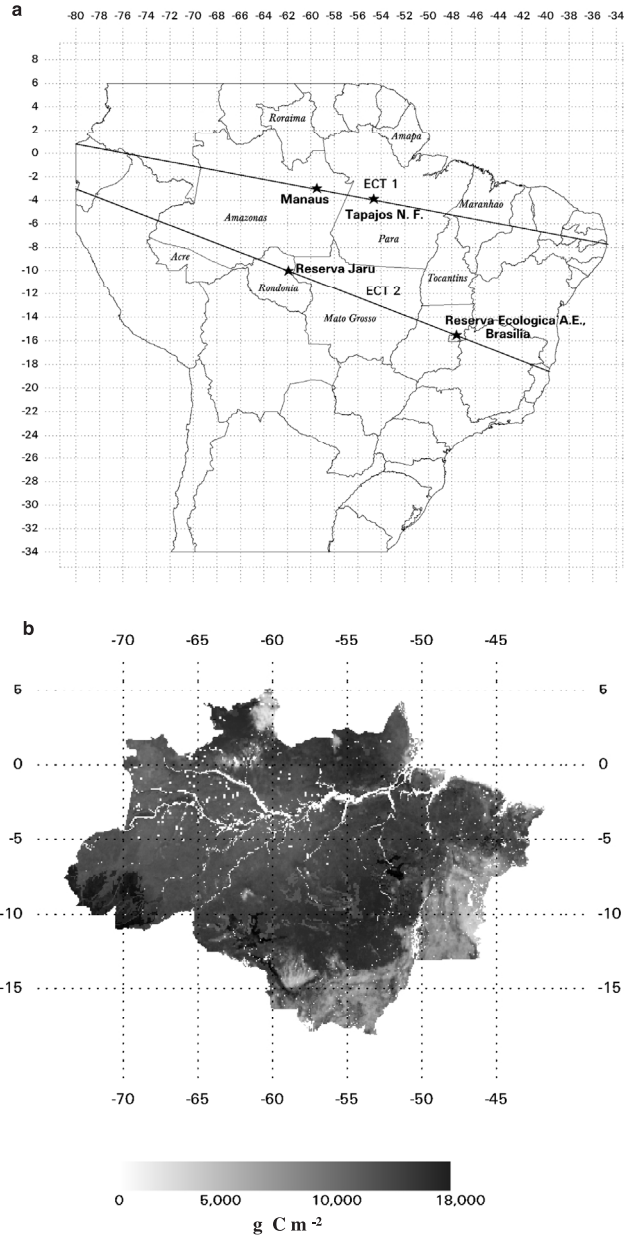


Figure 3. (a) States of the Legal Amazon in relation to ecoclimatic transects [ECT] across the study region [after LBA, 1996]. Site abbreviations are MSN for the INPA Tower Site, Manaus, Amazonas, STM for the Tapajós National Forest, Santarém, Pará, RND for the Reserva Jarú, Rondônia, and BSL for the Reserva Ecológica Aguas Emendadas, Brasília. (b) Regional distribution of aboveground biomass [leaf and wood] estimated from the NASA-CASA model for the early 1990s in states of the Legal Amazon. Units are g C m^{-2} . Reprinted from *Potter et al.* [2001a] with permission from Elsevier Science Ltd.

may act like sands in terms of water movement at low tensions, while holding water like clays at higher tensions. It is worth noting, however, that short-term variations and transient climate effects on soil moisture have minor influence over wood biomass predicted by the NASA-CASA model, since carbon from NPP is accumulated over many years (Table 1) to generate biomass pools in the model.

[17] Our ecosystem model must be initialized to obtain the beginning balance between predicted NPP and soil

carbon pools at all 8 km grid locations in the region. Conditions of near steady state carbon pools can be reached following the equivalent of 1200 monthly time steps in the initialization procedure.

[18] Following this initialization period of 100 years that equilibrated predicted carbon pools, we ran our model in a forward mode for nine successive years using the Brazil GIS data drivers (monthly climate) beginning from 1981 to 1982 conditions. NASA-CASA results for total amounts of

Table 2. Aboveground Biomass, Deforestation Rates, AVHRR Fire Counts, and Associated Biomass Burning Loss for 1992–1993 in States of the Legal Amazon

	Aboveground Biomass (Pg C) ^a	Rate of Deforestation ($10^4 \text{ km}^2 \text{ yr}^{-1}$) ^b	AVHRR 1 km Fire Count (10^4) in Primary Forest Areas ^c	AVHRR 1 km Fire Count (10^4) in Other Land Cover Areas ^d	Ratio of Area Deforested to Fire Counts ^e	Dry Matter Loss From Biomass Burning (10^9 kg yr^{-1}) ^f
Acre	2.36	0.048	0.117	0.045	0.41	11.8
Amapa	1.47	0.004	0.069	0.370	0.06	16.1
Amazonas	17.90	0.037	0.308	0.123	0.12	11.1
Maranhao	3.30	0.114	0.973	6.924	0.12	532.3
Mato Grosso	10.86	0.622	1.486	4.313	0.42	416.2
Pará	15.86	0.428	2.807	2.835	0.15	284.8
Rondônia	3.32	0.260	0.604	0.283	0.43	65.7
Roraima	2.49	0.024	0.149	0.462	0.16	17.6
Tocantins	2.19	0.033	0.008	3.852	4.40	223.6
Total for Legal Amazon	59.74	1.490	6.519	19.207	0.23	1579.2

^aFrom NASA-CASA model [Potter *et al.*, 2001a], summed over all land cover classes.

^bFrom the Brazilian Space Agency, INPE.

^cBased on GFP [Stroppiana *et al.*, 2000] in areas of the Legal Amazon defined by Stone *et al.* [1994] as tropical moist forest.

^dOther land cover classes with the majority of fire counts are cleared forests, secondary forests, and savanna/woodlands, according to land cover classification by Stone *et al.* [1994].

^eComputed as footnote b divided by footnote c.

^fIncludes only daily burning emissions, excludes postburning decomposition losses.

aboveground wood and leaf biomass across the states of the Legal Amazon (Figure 3a) for the early 1990s are 57.7 Pg (10^{15} g) wood C and 2.2 Pg leaf C (Table 2). The geographic distribution of NASA-CASA model forest biomass indicates that carbon amounts are highest in the seasonally dry forest areas of the eastern and southern states of Pará, Mato Grosso, and Rondônia states (Figure 3b), which is consistent with annual rates of NPP estimated by the model across forest types of Brazil [Potter *et al.*, 1998, 2001b]. Our model's predicted geographic distribution of forest biomass across the Legal Amazon region differs from that estimated by Houghton *et al.* [2000], who used stem-wood volume measurements assigned by land cover type or interpolated, mainly in that our model's predicted biomass amounts are relatively higher in the eastern and southern states of the region. The importance of this distinction between estimates of Amazon forest biomass distribution should be noted with respect to the most prevalent locations for deforestation and biomass burning in the region, which are also in the eastern and southern states [Alves, 1999].

2.2. Combustion and Emission Factor Estimates

[19] Our model results for biomass subject to burning (Table 2) were multiplied by a mean estimated combustion fraction of 0.95 for leaf material and a combustion fraction (C_F) of 0.45 for wood material, derived from Amazon forest slash burning studies [Kauffman *et al.*, 1995; Guild *et al.*, 1998; Sorrensen, 2000], to generate maps of the nominal burning emission fluxes of C for 365 consecutive days. We based these estimates for typical C_F values on studies that were conducted in the Amazon on small-holder properties, where all decisions as to which vegetation to burn, size of area slashed, location, and the timing of the slash and burn process (how to slash, how long to dry, when to burn) were entirely left to property owners. The initial distribution of biomass among tissue fractions (e.g., wood, leaf) and sizes may help explain differences found in C_F values among burning experiments [Fearnside *et al.*, 1999], and the estimated C_F values used in our analysis are fairly typical

of those reported in several other studies of tropical biomass burning [Hao and Lui, 1994; Graça *et al.*, 1999].

[20] The emission factors (e_f) we used in equation (1) were estimated by Scholes *et al.* [2000] based on a review of some 70 publications, a large fraction of which were produced as a result of International Geosphere–Biosphere Programme (IGBP) Biomass Burning Experiment (BIBEX) campaigns. It appears from this compilation of published e_f values that adequate data exist for most gas species for savanna fires but that for fires in tropical forests, only the emissions of some key gas species (e.g., CO, CH₄, NMHC, NO_x, SO₂) have been determined with fairly high confidence.

2.3. Satellite Data for Fire Area Detection

[21] Region-wide fire pixel counts from the AVHRR sensor can be used, in combination with our ecosystem model results for biomass, for detailed mapping of the daily abundance and spatial distribution of deforestation burning activities in a country like Brazil, provided that these relatively coarse resolution (1 km) satellite data are adjusted for several sources of fire detection bias. Pereira *et al.* [1991], for example, used AVHRR data to evaluate the accuracy of fire detection and burned area estimates in Brazil and found that all 1 km AVHRR-detected fires had corresponding Landsat TM fire scars but that actual fire sizes are overestimated by 43%, on average. More recently, Kaufman *et al.* [1998] reported that the typical size of the hottest areas of fires in Brazil are usually small (e.g., 0.005 km²), with a fire area distribution that peaks at between 0.2 km² and 1 km². Hence while it may be unreasonable to treat AVHRR fire counts as a reliable source for estimating the precise land area burned by fires in the Amazon, for our purposes, 1 km AVHRR fire count data can be used in combination with the NASA-CASA model mainly to detect the location and relative probability of daily biomass burning emissions of carbon to the atmosphere. Additional adjustments and methodology for actual area burned are described in the results that follow.

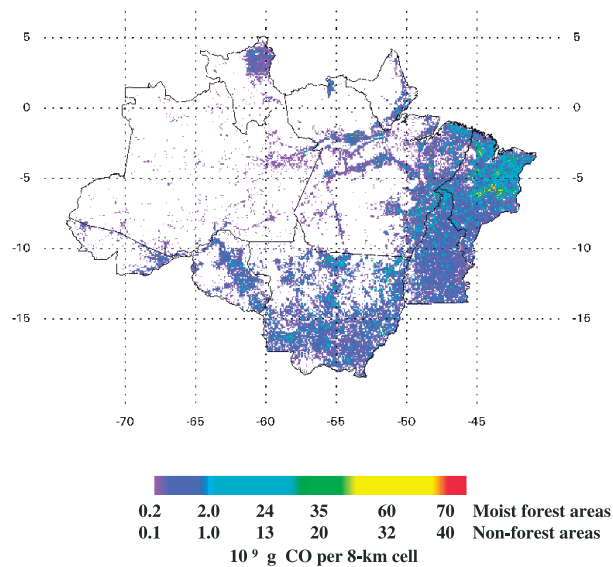


Figure 4. Regional distribution of total annual [1992–1993] carbon monoxide emissions from biomass burning over the Legal Amazon.

[22] The most readily available AVHRR fire data set for our analysis is the International Geosphere–Biosphere Programme (IGBP) Global Fire Product (GFP), which provides a consistent data set on daily fire counts at a global scale [Justice and Dowty, 1993; Dwyer et al., 1998; Stroppiana et al., 2000]. At this time, the GFP product is available only for an annual period spanning 1992–1993, which closely corresponds to the end of the NASA-CASA simulation period for this study. The GFP fire detection method is based on a selection of 1 km pixels that could potentially contain fires, with a confirmation procedure for the fire pixel classification by comparison of the pixel with its immediate geographic neighborhood [Flasse and Cecato, 1996]. The spectral basis for AVHRR fire detection algorithm is channel 3 (3.55–3.93 μm , mid IR), which is located near the optimum for high radiative emittance typical of vegetation fires [e.g., Langaas and Muirhead, 1988]. It is possible to detect fires burning over areas much smaller than the nominal 1 km AVHRR pixel size, because the total radiant emittance from a fire is disproportionately greater than that from a cooler background [Kennedy et al., 1994].

[23] There are several noteworthy interference problems with the AVHRR mid IR signal that must be overcome for accurate fire detection, including surface reflection of solar radiation in the 3.75 μm band, transmission effects of atmospheric water vapor, subresolution clouds, and viewing geometry (i.e., Sun glint effect) of the AVHRR sensor [Gregoire, 1993]. To remove most effects of cloud reflectances, masking is normally performed before applying fire detection algorithms. This is accomplished using the added channel 4 temperature to eliminate false detection from cool clouds that are highly reflective in the 3.8 μm band. It is acknowledged then that the cloud-masking step leaves some actual ground fires undetected in the GFP data sets. On the other hand, wherever the GFP indicates high fire counts, these pixels should accurately represent cloud-free measurements of daily surface fire activity.

[24] To combine AVHRR fire counts with the NASA-CASA model’s predicted biomass values for the Legal Amazon, we first aggregated the 1 km GFP fire count data to the resolution of our 8 km regional grid. All Amazon fires detected in the GFP record during 1992–1993 were counted in order to capture a full year of daily burning activity at each 8 km pixel location. To next generate a “nominal” biomass emission loss from each 8 km grid cell in the Legal Amazon region, we multiplied both leaf biomass and wood biomass values, as produced from early 1990s NASA-CASA model simulation, by the number of 1 km fire counts per 8 km cell per day of the 1992–1993 annual period.

[25] It is necessary next to “scale-down” our nominal burning emission fluxes, which are evidently biased toward area overestimation in 1 km fire counts. An adjustment is required to make areas inferred from the GFP fire counts closely match deforestation area rates reported by the Brazilian Space Agency, INPE, which based its estimates on analysis of Landsat imagery for the 1990s [Alves, 1999]. This is accomplished by comparison of the annual (1992–1993) total 1 km fire pixel counts in primary forest areas delineated by Stone et al. [1994] per state of the Legal Amazon to state-by-state INPE deforestation area estimates for 1992 (reported, for example, by Kaufman et al. [1998] and Houghton et al. [2000]). This comparison generates a set of ratio conversion factors (Table 2), which can then be used to proportionally reduce the nominal burning C emission estimates derived from total 1 km AVHRR fire counts. We find that the region-wide ratio of INPE-estimated area deforested divided by 1 km forest fire is 0.23.

[26] According to the GFP record for 1992–1993, 75% of all fire counts in the Legal Amazon region were in areas outside the primary moist forest zone. These areas have cover types delineated by Stone et al. [1994] as mainly (60%) seasonal deciduous woodlands and secondary forests, presumably interspersed with areas of cattle pasture. The remaining 15% of fires detected outside the primary

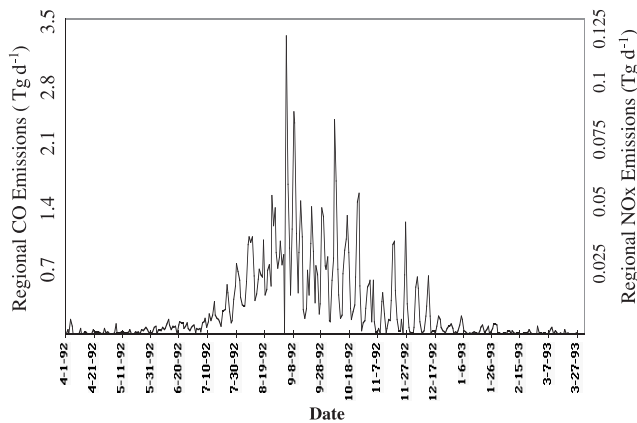


Figure 5. Carbon monoxide and nitrogen oxide emissions resulting from biomass burning for days of the year 1992–1993, summed over the entire Legal Amazon region.

forest zone were chiefly in savanna/woodlands (cerrado). On the basis of previous Landsat image analyses in such areas outside the primary forest zone [Setzer and Pereira, 1991], we therefore assumed a ratio conversion factor for the quantity [burned area; 1 km fire pixel count] of 0.73 for these cover types.

3. Regional Emission Estimates

[27] Using adjustments of GFP fire counts to be consistent with the 1992–1993 INPE deforestation area estimates and in burned cerrado areas, we calculate the annual direct burning source of gross C emissions in the entire Legal Amazon to be $0.71 \text{ Pg C yr}^{-1}$, which represents about 1580 Tg yr^{-1} dry biomass burned (Table 2). More than 85% of this total emission flux was mapped to areas outside of moist primary forest areas. The regional distribution of biomass burning emissions shows deforestation and burning emissions to be highest in the states of Maranhao and Tocantins mainly from burning outside of moist forest areas, and in Para and Mato Grosso with important contributions from primary forest cutting and burning (Figure 4).

[28] Our predicted daily flux of trace gases to the atmosphere directly from Amazon deforestation fires and other biomass burning shows emissions increasing rapidly at the end of July, reaching peak levels in early September, and decreasing gradually until mid-December 1992 (Figure 5). Day-to-day variability in emissions is a function solely of observed fire counts from the GFP over the region. Maximum daily burning fluxes to the atmosphere over the entire Brazilian Legal Amazon were estimated at slightly more than 3 Tg CO d^{-1} and $0.1 \text{ Tg NO}_x \text{ d}^{-1}$ in early September 1992.

[29] As implied by a comparison of gas emission factors (Table 3), our results suggest that total annual loading of reactive trace gases are dominated by carbon monoxide burning fluxes at nearly $102 \text{ Tg CO yr}^{-1}$. Next, in decreasing order, we estimate annual burning emissions of 11.1 Tg total particulate matter (TPM), 6.7 Tg NMHC, 4.2 Tg CH_4 , and 3.5 Tg NO_x from the Legal Amazon. For all emission species, burning emission sources from the states of Mar-

anhao and Mato Grosso together contribute over half of the regional flux total for the Legal Amazon.

4. Discussion

[30] Our model estimate of 1580 Tg yr^{-1} dry biomass burned in the Legal Amazon of Brazil is within 7% of the estimate of 1690 Tg yr^{-1} by Hao and Lui [1994] for a slightly larger area of tropical South America. In lieu of using satellite data sources, Hao and Lui [1994] used the best available ground-based forest inventory data to compute biomass available for burning in a number of different forest, savanna, and agricultural systems, together with census data sources for areas annually burned over a $5^\circ \times 5^\circ$ regional grid. Our regional results are also in close agreement with those of Hao and Lui [1994] in that just over 85% of total burning emissions can be mapped to areas outside of moist primary forest areas of the Amazon. The close agreement of these two very different approaches (satellite based and inventory/census based) to estimate biomass burning emissions over the Amazon region is a practical validation of our overall modeling methodology outlined in Figure 1.

[31] From the global perspective, Scholes *et al.* [2000] estimated that biomass burning worldwide results in emissions that total nearly $600 \text{ Tg CO yr}^{-1}$, whereas hydrocarbon (methane plus NMHC) emissions account for about 50 Tg C , and carbonaceous particulate matter emissions about 38 Tg C in organic compounds. Comparison of our model emission results from 1992 to 1993 suggests that the Brazilian Amazon region is a source of between one fifth and one third for each of these global carbon-based emission fluxes to the atmosphere. Using a high-end flux for global biomass burning of $12 \text{ Tg NO}_x \text{ yr}^{-1}$ estimated by Crutzen and Andreae [1990], the contribution level of about one fourth of global yearly emissions holds true also for our estimated NO_x burning emissions from sources in the Legal Amazon region. Although SO_2 emissions from biomass burning (e.g., $0.6 \text{ Tg SO}_2 \text{ yr}^{-1}$ for the Legal Amazon) may make only a small contribution to the atmospheric sulfur budget, it is important to quantify all possible sources of SO_2 -derived aerosols for impacts on global energy balance.

Table 3. Biomass Burning Emission Totals^a (Tg yr^{-1}) for 1992–1993 in States of the Legal Amazon^b

	CO	CH_4	NMHC	NO_x	SO_2	TPM
Moist forest e_f	106.0	<0.1	8.4	1.5	0.57	8.0
Nonforest e_f	58.0	2.0	3.6	2.3	0.35	6.9
Acre	1.0	0.1	0.1	<0.1	<0.1	0.1
Amapa	1.0	<0.1	0.1	<0.1	<0.1	0.1
Amazonas	0.8	<0.1	0.1	<0.1	<0.1	0.1
Maranhao	31.5	1.1	2.0	1.2	0.2	3.7
Mato Grosso	28.5	1.3	1.9	0.9	0.2	3.0
Para	19.2	0.8	1.3	0.6	0.1	2.0
Rondonia	5.6	0.3	0.4	0.1	<0.1	0.5
Roraima	1.1	<0.1	0.1	<0.1	<0.1	0.1
Tocantins	13.0	0.5	0.8	0.5	0.1	1.5
Total for Legal Amazon	101.7	4.2	6.7	3.5	0.6	11.1

^aBiomass burning emission totals is expressed in Tg yr^{-1} .

^bEmission factor (e_f) estimates (g kg^{-1} dry matter) derived from Scholes *et al.* [2000] are shown immediately below each gas species.

Table 4. Summary of Error Estimates for Terms in Equation (1) Used to Predict Tropical Biomass Burning Emissions of Atmospheric Trace Gases^a

Variable	Error Estimate		Reference
	Moist Forest	Nonforest	
B	±60%	TBD	<i>Houghton et al.</i> [2000]
C_F	±6%	±5%	<i>Scholes et al.</i> [2000]
e_f	±20–40%	±20–30%	<i>Scholes et al.</i> [2000]
A	TBD	TBD	<i>Setzer and Pereira</i> [1991]; <i>Alves</i> [1999]

^a B is the biomass over the region, C_F is the biomass combustion fraction, e_f is the emission factor (flaming and/or smoldering) associated with emissions of CO, CH₄, and NMHC from tropical biomass burning, A is the area burned over the region in a single year. TBD is “to be determined” through subsequent analysis using ground-based verification of Landsat or other satellite products for distribution of biomass and burned areas in Amazon ecosystems across the region.

[32] In all regional modeling studies such as this one, assumptions must be made with respect to the uncertainties in model variables, such as those shown in equation (1). As one way to quantify the confidence in current burning emission estimates for the region, information on error ranges for model variables can be collected from several reviews of region-wide or global ecosystem and burning emission studies. Although the error estimation matrix we have compiled (Table 4) cannot be completed without further analysis, using extensive ground-based verification of Landsat or other satellite products for distribution of biomass and burned areas in Amazon ecosystems across the region, we can identify several sources of high uncertainty in published error ranges for variables in our equation (1). Estimates of aboveground biomass over the region remain among the most poorly constrained of these variables [*Houghton et al.*, 2000]. Progress in narrowing this high level of uncertainty in regional biomass subject to burning may require advances in the use and verification of lidar (light detection and ranging) technology together with other satellite data from optical and radar sensors. The next largest known source of error in the emissions equation is the burning emission factor for each individual trace gas [*Scholes et al.*, 2000], although this type of information is becoming more commonly available for tabulation from field-based experiments. In contrast, the biomass combustion fraction term already appears to be a relatively well-constrained variable in the burning emissions equation. Overall, it appears that the minimum error estimate for the trace gas emission rates we report in this study, assuming that the majority of emissions comes from areas outside the moist forest zones of the Legal Amazon region, would be on the order of ±30%.

[33] Models of atmospheric chemistry are needed to predict the global distribution of sources, concentrations, and sinks of trace gases and particles that are either radiatively active or are precursors of such species. Enhanced versions of these models will be used to study the future of global air pollution impacts or to estimate the radiative forcing due to anthropogenic gases and aerosols, including biomass burning emissions. However, because measurements of trace gas emission sources and aerosols are sparse, tropospheric chemistry models require continuously improved forcing fields for most gas sources and sinks. The satellite-based methodology described in this

paper to generate daily, high spatial resolution emission fluxes of most major trace gas from biomass burning can be readily expanded to other regions of the tropical zone to help fill this gap in data inputs to atmospheric chemistry models.

[34] **Acknowledgments.** We thank three anonymous reviewers for helpful comments on an earlier version of the manuscript. This work was supported by grants from NASA programs in Land Surface Hydrology and the Large-Scale Biosphere-Atmosphere Experiment in Amazonia (LBA-Ecology Component). Data set maps for biomass burning emissions may be obtained upon request from the primary author (cpotter@mail.arc.nasa.gov).

References

- Aber, J. D., and J. M. Melillo, *Terrestrial Ecosystems*, 429 pp., Saunders Coll., Philadelphia, Pa., 1991.
- Agbu, P. A., and M. E. James, *NOAA/NASA Pathfinder AVHRR Land Data Set User's Manual*, Goddard Distrib. Active Arch. Cent., NASA Goddard Space Flight Cent., Greenbelt, Md., 1994.
- Alves, D. S., Geographical patterns of deforestation in the 1991–1996 period, in *Patterns and Processes of Land Use and Forest Change in the Amazon*, Univ. of FL., Gainesville, Fla., 1999.
- Artaxo, P., H. Storms, F. Bruynseels, R. V. Grieken, and W. Maenhaut, Composition and sources of aerosols from the Amazon Basin, *J. Geophys. Res.*, **93**, 1605–1615, 1988.
- Bishop, J. K. B., and W. B. Rossow, Spatial and temporal variability of global surface solar irradiance, *J. Geophys. Res.*, **96**, 16,839–16,858, 1991.
- Cannell, M. G. R., *World Forest Biomass and Primary Production Data*, Academic, San Diego, Calif., 1982.
- Ciais, P., P. P. Tans, J. W. C. White, M. Trolier, R. J. Francey, J. A. Berry, D. R. Randall, P. J. Sellers, J. G. Collatz, and D. S. Schimel, Partitioning of ocean and land uptake of CO₂ as inferred by ¹³C measurements from the NOAA Climate monitoring and diagnostics laboratory global air sampling network, *J. Geophys. Res.*, **100**, 5051–5070, 1995.
- Crutzen, P. J., Overview of tropospheric chemistry: Developments during the past quarter century and a look ahead, *Faraday Discuss.*, **100**, 1–21, 1995.
- Crutzen, P. J., and M. O. Andreae, Biomass burning in the tropics: Impact on atmospheric chemistry and biogeochemical cycles, *Science*, **250**, 1669–1678, 1990.
- DeFries, R., and J. Townshend, NDVI-derived land cover classification at global scales, *Int. J. Remote Sens.*, **15**, 3567–3586, 1994.
- Dwyer, E., J.-M. Grégoire, and J. P. Malingreau, A global analysis of vegetation fires using satellite images: Spatial and temporal dynamics, *Ambio*, **27**, 175–181, 1998.
- Fearnside, P. M., P. M. L. A. Graça, N. Leal Filho, F. J. A. Rodrigues, and J. M. Robinson, Tropical forest burning in Brazilian Amazonia: Measurements of biomass, burning efficiency and charcoal formation at Altamira, Pará, *For. Ecol. Manage.*, **123**, 65–79, 1990.
- Flasse, S. P., and P. S. Ceccato, A contextual algorithm for AVHRR fire detection, *Int. J. Remote Sens.*, **17**, 419–424, 1996.
- Galanter, M., H. Levy II, and G. R. Carmichael, Impacts of biomass burning on tropospheric CO, NO_x and O₃, *J. Geophys. Res.*, **105**, 6633–6653, 2000.
- Gleeson, S. K., and D. Tilman, Allocation and the transient dynamics of succession on poor soils, *Ecology*, **71**, 1144–1155, 1990.
- Graça, P. M. L. A., P. M. Fearnside, and C. C. Cerri, Burning of Amazonian forest in Ariquemes, Rondônia, Brazil: Biomass, charcoal formation and burning efficiency, *For. Ecol. Manage.*, **120**, 179–191, 1999.
- Grégoire, J.-M., Use of AVHRR for the study of vegetation fires in Africa: Fire Management Perspectives, Euro courses, in *Advances in the Use of AVHRR Data for Land Applications*, Publication of the European Commission, Ispra, Italy, 1993.
- Guild, L. S., J. B. Kauffman, L. J. Ellingson, D. L. Cummings, and E. A. Castro, Dynamics associated with total aboveground biomass, C, nutrient pools, and biomass burning of primary forest and pasture in Rondônia, Brazil, during SCAR-B, *J. Geophys. Res.*, **103**, 32,091–32,100, 1998.
- Hao, W.-M., and M. H. Lui, Spatial and temporal distribution of tropical biomass burning, *Global Biogeochem. Cycles*, **8**, 495–503, 1994.
- Houghton, R. A., D. L. Skole, C. A. Nobre, J. L. Hackler, K. T. Lawrence, and W. H. Chomentowski, Annual fluxes of carbon from deforestation and regrowth in the Brazilian Amazon, *Nature*, **403**, 301–304, 2000.
- IBGE, *Anu. Estatístico do Brasil*, vol. 51, pp. 1–1024, Instituto Brasileiro de Geografia e Estatística, Rio de Janeiro, Brazil, 1991.
- Jacob, D. J., et al., The origin of ozone and NO_x in the tropical troposphere:

- A photochemical analysis of aircraft observations over the South Atlantic basin, *J. Geophys. Res.*, *101*, 24,235–24,250, 1996.
- Justice, C. O., and P. Dowty, IGBP-DIS satellite fire detection algorithm workshop technical report, IGBP-DIS Work. Pap. 9, 88 pp., NASA Goodard Space Flight Cent., Greenbelt, Md., 1993.
- Kauffman, J. B., D. L. Cummings, D. E. Ward, and R. Babbitt, Fire in the Brazilian Amazon: Biomass, nutrient pools, and losses in slashed primary forests, *Oecologia*, *104*, 397–408, 1995.
- Kaufman, Y. J., et al., Smoke, Clouds, and Radiation-Brazil (SCAR-B) experiment, *J. Geophys. Res.*, *103*, 31,783–31,808, 1998.
- Kennedy, P. J., A. S. Belward, and J.-M. Gregoire, An improved approach to fire monitoring in West Africa using AVHRR data, *Int. J. Remote Sens.*, *15*, 2235–2255, 1994.
- Langaas, S., and K. Muirhead, Monitoring bushfires in West Africa by weather satellite, *Int. Symp. Remote Sens. Environ.*, *2*, 253–268, 1988.
- Lobert, J. M., D. H. Scharffe, W. Hao, T. A. Kuhlbusch, R. Seuwen, P. Wameck, and P. J. Crutzen, Experimental evaluation of biomass burning emissions: Nitrogen and carbon containing compounds, in *Global Biomass Burning: Atmospheric, Climatic, and Biospheric Implications*, edited by J. S. Levine, 568 pp., MIT Press, Cambridge, Mass., 1991.
- Los, S. O., C. O. Justice, and C. J. Tucker, A global 1 × 1 NDVI data set for climate studies derived from the GIMMS continental NDVI data, *Int. J. Remote Sens.*, *15*, 3493–3518, 1994.
- Lusk, C. H., O. Contreras, and J. Figueroa, Growth, biomass allocation and plant nitrogen concentration in Chilean temperate rainforest tree seedlings: Effects of nutrient availability, *Oecologia*, *109*, 49–58, 1997.
- Ministério das Minas e Energia (MME), *Projeto RADAMBRASIL*, Rio de Janeiro, Brazil, 1981.
- Nepstad, D. C., et al., Large-scale impoverishment of Amazonian forests by logging and fire, *Nature*, *398*, 505–508, 1999.
- New, M., M. Hulme, and P. Jones, Representing twentieth century space-time climate variability. II, Development of 1901–1996 monthly grids of terrestrial surface climate, *J. Clim.*, *13*, 2217–2238, 2000.
- Pereira, A. C., Jr., A. W. Setzer, and J. R. dos Santos, Fire estimates in savannas of central Brazil with thermal AVHRR/NOAA calibrated by TM/Landsat, paper presented at the International Symposium on Remote Sensing of Environment, Rio de Janeiro, Brazil, 27–31 May 1991.
- Potter, C. S., Terrestrial biomass and the effects of deforestation on the global carbon cycle, *BioScience*, *49*, 769–778, 1999.
- Potter, C. S., and S. A. Klooster, Global model estimates of carbon and nitrogen storage in litter and soil pools: Response to change in vegetation quality and biomass allocation, *Tellus, Ser. B*, *49*, 1–17, 1997.
- Potter, C. S., and S. A. Klooster, Dynamic global vegetation modeling (DGVM) for prediction of plant functional types and biogenic trace gas fluxes, *Global Ecol. Biogeogr. Lett.*, *8*, 473–488, 1999a.
- Potter, C. S., and S. A. Klooster, Detecting a terrestrial biosphere sink for carbon dioxide: Interannual ecosystem modeling for the mid-1980s, *Clim. Change*, *42*, 489–503, 1999b.
- Potter, C. S., J. T. Randerson, C. B. Field, P. A. Matson, P. M. Vitousek, H. A. Mooney, and S. A. Klooster, Terrestrial ecosystem production: A process model based on global satellite and surface data, *Global Biogeochem. Cycles*, *7*, 811–841, 1993.
- Potter, C. S., E. A. Davidson, S. A. Klooster, D. C. Nepstad, G. H. deNeyreiros, and V. Brooks, Regional application of an ecosystem production model for studies of biogeochemistry in Brazilian Amazonia, *Global Change Biol.*, *4*, 315–334, 1998.
- Potter, C. S., V. Brooks-Genovese, S. A. Klooster, M. Bobo, and A. Torregrosa, Biomass burning losses of carbon estimated from ecosystem modeling and satellite data analysis for the Brazilian Amazon region, *Atmos. Environ.*, *35*, 1773–1781, 2001a.
- Potter, C. S., S. Klooster, C. R. deCarvalho, V. Brooks-Genovese, A. Torregrosa, J. Dungan, M. Bobo, and J. Coughlan, Modeling seasonal and interannual variability in ecosystem carbon cycling for the Brazilian Amazon region, *J. Geophys. Res.*, *106*, 10,423–10,446, 2001b.
- Priestly, C. H. B., and R. J. Taylor, On the assessment of surface heat flux and evaporation using large-scale parameters, *Mon. Weather Rev.*, *100*, 81–92, 1972.
- Prins, E. M., J. M. Feltz, W. P. Menzel, and D. E. Ward, An overview of GOES-8 diurnal fire and smoke results for SCAR-B and 1995 fire season in South America, *J. Geophys. Res.*, *103*, 31,821–31,830, 1998.
- Redente, E. F., J. E. Friedlander, and T. McLendon, Response of early and late successional species to nutrient gradients, *Plant Soil*, *140*, 127–135, 1992.
- Running, S. W., and S. T. Gower, FOREST-BGC, A general model of forest ecosystem processes for regional applications, II, Dynamic carbon allocation and nitrogen budgets, *Tree Physiol.*, *9*, 147–160, 1991.
- Scholes, M., P. Matrai, K. Smith, M. Andreae, and A. Guenther, Biosphere-atmosphere interactions, in *Atmospheric Chemistry in a Changing World*, Cambridge Univ. Press, New York, 2000.
- Seiler, W., and P. J. Crutzen, Estimates of gross and net fluxes of carbon between the biosphere and atmosphere from biomass burning, *Clim. Change*, *2*, 207–247, 1980.
- Sellers, P. J., C. J. Tucker, G. J. Collatz, S. O. Los, C. O. Justice, D. A. Dazlich, and D. A. Randall, A global 1x1 NDVI data set for climate studies, Part 2, The generation of global fields of terrestrial biophysical parameters from the NDVI, *Int. J. Remote Sens.*, *15*, 3519–3545, 1994.
- Setzer, A. W., and A. C. Pereira Jr., Amazon biomass burnings in 1987 and an estimate of their tropospheric emissions, *Ambio*, *20*, 19–22, 1991.
- Sorensen, C. L., Linking smallholder land use and fire activity: Examining biomass burning in the Brazilian Lower Amazon, *For. Ecol. Manage.*, *128*, 11–25, 2000.
- Stone, T. A., P. Schlesinger, R. A. Houghton, and G. M. Woodwell, A map of vegetation of South America based on satellite imagery, *Photogramm. Eng. Remote Sens.*, *60*, 541–551, 1994.
- Stroppiana, D., S. Pinnock, and J.-M. Grégoire, The global fire product: Daily fire occurrence from April 1992 to December 1993 derived from NOAA-AVHRR data, *Int. J. Remote Sens.*, *21*, 1279–1288, 2000.
- Terborgh, J., C. N. Flores, P. Mueller, and L. Davenport, Estimating the ages of successional stands of tropical trees from growth increments, *J. Trop. Ecol.*, *14*, 833–856, 1997.
- Thompson, A. M., K. E. Pickering, D. P. McNamara, M. R. Schoeberl, R. D. Hudson, J. H. Kim, E. V. Browell, V. W. J. H. Kirchhoff, and D. Nganga, Where did tropospheric ozone over southern Africa and the tropical Atlantic come from in October 1992? Insights from TOMS, GTE TRACE-A, and SAFARI 1992, *J. Geophys. Res.*, *101*, 24,251–24,278, 1996.
- Ward, D. E., W.-M. Hao, R. A. Susott, R. A. Babbitt, R. W. Shea, J. B. Kauffman, and C. O. Justice, Effect of fuel composition on combustion efficiency and emission factors for African savanna ecosystems, *J. Geophys. Res.*, *101*, 23,569–23,576, 1996.
- Wilson, S. D., and D. Tilman, Components of plant competition along an experimental gradient of nitrogen availability, *Ecology*, *72*, 1050–1065, 1991.
- Yokelson, R. J., R. Susott, D. E. Ward, J. Reardon, and D. W. T. Griffith, Emissions from smoldering combustion of biomass measured by open-path Fourier transform infrared spectroscopy, *J. Geophys. Res.*, *102*, 18,865–18,877, 1997.

C. Potter, Ecosystem Science and Technology Branch, NASA Ames Research Center, Mail Stop 242-4, Moffett Field, CA 94035, USA. (cpotter@gaia.arc.nasa.gov)

V. Brooks-Genovese, S. Klooster, and A. Torregrosa, Earth System Science and Policy, California State University Monterey Bay, Seaside, CA USA.